Araştırma Makalesi / Research Article

The Effect of Pressure to the Crystallization and Glass Transition Temperature of Liquid PdSi Alloy Modelled with Quantum Sutton-Chen Potential

Sefa KAZANC[1], Canan AKSU CANBAY[2*]

[1]*Firat University, Department of Mathematics and Science, 23119, Elazig, Turkey*
[2]*Firat University, Department of Physics, Elazig 23169, Turkey*
(ORCID: 0000-0002-8896-8571) (ORCID: 0000-0002-5151-4576)

Abstract
In this work, the effect of pressure on the crystallization (T_c) and glass transition (T_g) temperatures of a modelled PdSi liquid alloy was investigated for different cooling rates by using Quantum Sutton Chen(K-SC) potential which is used to determine the interactions between atoms. It was determined that at the cooling rates of $2{,}5x10^{11}$ K/s and $2{,}5x10^{12}$ K/s the alloy system in liquid phase transformed into crystal and amorphous phase, respectively. The glass transition temperature was defined by the Wendt-Abraham parameter and radial distribution function (RDF) peaks. It was concluded that the increment of pressure led to an increase in the crystallization and glass transition temperatures and the ratio of T_g/T_m resulted in an improvement of the glass forming ability.

Keywords: Quantum Sutton Chen, Glass transition temperature, Crystallization temperature, PdSi alloy.

Quantum Sutton-Chen Potansiyeli ile Modellenen Sıvı PdSi Alaşımının Kristalizasyon ve Camsı Geçiş Sıcaklığına Basıncın Etkisi

Öz
Bu çalışmada atomlar arasındaki etkileşmelerin belirlenmesinde Kuantum Sutton Chen (K-SC) potansiyel fonksiyonu kullanılarak farklı soğutma hızları için model PdSi sıvı alaşımının kristallenme (Tc) ve camsı geçiş sıcaklıklarına (Tg) basıncınetkisi incelendi. $2{,}5x10^{11}$ K/s ve $2{,}5x10^{12}$K/s soğutma hızlarında sıvı fazdaki alaşım sisteminin sırasıyla kristal ve amorf faza dönüştüğü tespit edildi. Camsı geçiş sıcaklığı, Wendt-Abraham parametresi ve radyal dağılım fonksiyonu (RDF) piklerinden belirlendi. Basınç artışınınkristallenme, camsı geçiş sıcaklığıve Tg/Tm oranınıyükselterek camsı oluşum kabiliyetini arttırdığı tespit edildi.

Anahtar kelimeler: Kuantum Sutton Chen, Cam geçiş sıcaklığı, Kristalleşme sıcaklığı, PdSi alaşımı.

1.Introduction

The glassy metals (also known as metallic glasses or amorphous metals) are attractive materials due to their wear, high corrosion resistance, hardness and superior magnetic properties [1, 2]. The first metallic glass was first synthesized by fast cooling of $Au_{75}Si_{25}$ alloy from liquid phase by Duwez et al.in 1960 [3]. Amorphous structures are generally obtained by cooling the material from the liquid phase with a cooling rate (10^6-10^{12} K/s) which will not allow the crystalline phase to nucleation and grow [4, 5]. Droplet cooling and piston anvil method [6], blow molding method [7], levitation melting and casting method [8] are the most commonly used methods in the production of metallic glasses. In addition to these, milling [9], mechanical alloying [10], laser and electron bombardment [11] methods are also used in the manufacture of metallic vitreous materials in frequently. The metals in the liquid phase may solidify in crystalline or amorphous form depending on the cooling rate. The elements and alloys

*Sorumlu yazar: caksu@firat.edu.tr
Geliş Tarihi:08.05.2019, Kabul Tarihi: 19.09.2019

solidified in amorphous form have a thermodynamically semi-stable structure [12].The best metallic glasses are obtained from zirconium and palladium alloys. Composite armors, aircraft and ship parts, biomedical materials, electrical transformers, solar and wind panels are the application areas where metallic glasses are used [13]. The difficulties in their production due to weakness of their plastic deformations bring into being the biggest disadvantage of these materials. In the recent research made on glassy metals, the necessary factors were determined for glass forming.

The ratio of glass transition (T_g) temperature over melting temperature (T_m) which is reduced glass temperature ($T_{rg}=T_g/T_m$)can be used as a benchmark to determine the glass forming ability of an element or alloy [3]. For pure metals T_{rg}=0,25 and for alloy systems it can take the values between 0.5 and 0.8 [3, 14]. It is very important to know the microscopic mechanism of the formation of crystalline and amorphous structure from liquid phase. However, to study the effect of pressure experimentally on glass transition temperature is quite difficult. Recently, through the development of computer technology, researchers have been studied the effect of the applied pressure in the process of fast-cooling from the liquid phase theoretically by using the molecular dynamic simulation techniques [15-17]. There are effective simulation techniques that provide an understanding of the physical structure and properties of the systems in atomic scale. One of these techniques, the Molecular Dynamic (MD) simulation method, is widely used to study the structural and thermodynamic properties of high-tech materials such as intermetallic alloys, metallic glasses, semiconductors, polymers and nanostructures [18-21].

For a system composed of *N* particles, solving the equations of motion determined by the Lagrange or Hamiltonian functions by means of an appropriate numerical algorithm constitutes the basis of classical MD simulation method. [22, 23]. In MD simulation studies, determining the correct potential energy function that defines interatomic interactions for the system to be examined is extremely important for the obtained results to be consistent with the experimental data.

On the other hand, the determination of potential energy parameters for different atomic types in the modelling of alloy systems isa problem faced in MD studies [18-21]. One of the effective potential functions used in the modelling of both monatomic and alloy systems is the Embedded Atom Method, which involves many-body interactions proposed by Daw and Baskes [24]. Furthermore, varied types of function have been developed by Vother-Chen [25], Finnis-Sinclair [26] and Sutton-Chen [27] to model different metallic systems [28, 29].

The systems to be examined can be modelled by first-principles methods more realistically. However, low number of particles and high-speed computers for calculations are necessary [30]. The K-SC potential determined by fitting the parameters to the properties of first-principles has been used successfully in examining the glassy formation, crystallization phenomena and surface properties of metallic systems and in the modelling of clustered structures and nanowires [14].

In this study, the liquid PdSi alloy was modelled by using the potential function of Quantum Sutton-Chen (K-SC) [28] and the effect of pressure on the phase transformation temperatures was investigated under different cooling rates. The temperatures of transitions from alloy system modelled in liquid phase to the crystal and amorphous structures obtained under different cooling rates were determined from the discontinuities in the cohesive energy and the Wendt-Abraham parameter, respectively. Furthermore, it was tried to identify the structure of the modelled alloy system by using the Radial Distribution Functions (RDF) obtained under different temperature and pressure values.

2. Material and Methods

The solution of the motion equation of the system to be modelled obtained from the Lagrange function by a suitable numerical algorithm forms the basis of MD simulation. The Lagrange function of MD cell composed of *N* atoms allowed to change shape and volume [31, 32] is given as;

$$L_{PR}\left(\mathbf{r}^N, \dot{\mathbf{r}}^N, \mathbf{h}, \dot{\mathbf{h}}\right) = \frac{1}{2}\sum_{i=1}^{N} m_i\left(\dot{\mathbf{s}}_i^t \mathrm{G}\dot{\mathbf{s}}_i\right) - \sum_{i=1}^{N}\sum_{j>i}^{N} \phi\left(\left|\mathbf{h}\mathbf{s}_{ij}\right|\right) + \frac{1}{2}M\mathrm{Tr}\left(\dot{\mathbf{h}}^t\dot{\mathbf{h}}\right) - P_{ext}V \qquad (1)$$

Here, m_i is the mass of the *i* particle; s_i is the coordinate of the i^{th} atom that can take the values between 0 and 1;**a**, **b**, and **c** representing the computational cell axes constitute the **h**=(**a**, **b**, **c**) matrix; and **G**refers to the metric tensor having the value of $\mathbf{h}^t\mathbf{h}$. Besides, *M* having an arbitrary value denotes the mass of

the computational cell; P_{ext} refers to the value of external pressure; and V obtained from taking the determinant of **h** matrix is the volume of the MD cell. From Equation (1) the equations of motion of the system were found as;

$$\ddot{\mathbf{s}}_i = -\frac{1}{m_i}\mathbf{F}_i - \mathbf{G}^{-1}\dot{\mathbf{G}}\dot{\mathbf{s}}_i \tag{2}$$

$$\ddot{\mathbf{h}} = M^{-1}(\Pi - \mathbf{I}P_{ext})\sigma \tag{3}$$

In these equations, σ=(**b**×**c**, **c**×**a**, **a**×**b**) and **Π** refers to the microscopic stress tensor. The clear express of microscopic stress tensor is given as below;

$$\mathbf{\Pi} = V^{-1}\left[\sum_{i=1}^{N} m_i \boldsymbol{v}_i \cdot \boldsymbol{v}_i - \sum_{i=1}^{N}\sum_{j>i}^{N} \frac{F_{ij}}{r_{ij}}\,\mathbf{r}_i \cdot \mathbf{r}_i\right] \tag{4}$$

2.1. Potential Energy Function

In this study, in order to determine the physical interactions between the atoms of the binary alloy system, the K-SC potential, a type of the Embedded Atom Method (EAM) involving many-body interactions, was used. According to this EAM method, the total energy of a system consisting of N atoms and containing two different atomic types such as a and b is expressed as;

$$E_T^{SC} = \left\{\frac{1}{2}\sum_{i^a,j^a}^{N^a}\varepsilon_a\left(\frac{A_a}{r_{ij}}\right)^{n_a} - \sum_{i^a}^{N^a}\varepsilon_a c_a\left[\sum_j\left(\frac{A_a}{r_{ij}}\right)^{m_a}\right]^{1/2}\right\} +$$

$$\left\{\frac{1}{2}\sum_{i^b,j^b}^{N^b}\varepsilon_b\left(\frac{A_b}{r_{ij}}\right)^{n_b} - \sum_{i^b}^{N^b}\varepsilon_b c_b\left[\sum_j\left(\frac{A_b}{r_{ij}}\right)^{m_b}\right]^{1/2}\right\} + \tag{5}$$

$$\frac{1}{2}\sum_{i^a,j^b}^{N^{ab}}\varepsilon_{ab}\left(\frac{A_{ab}}{r_{ij}}\right)^{n_{ab}} + \frac{1}{2}\sum_{i^b,j^a}^{N^{ba}}\varepsilon_{ba}\left(\frac{A_{ba}}{r_{ij}}\right)^{n_{ba}}$$

Here, i^a and i^b represent the sums over all a and b type atoms. In calculations, the potential parameters used to determine the interactions between different types of atoms that form the alloy system were proposed by Lorentz-Berthelet [18] following as below;

$$A_{ij} = A_{ji} = \frac{A_i + A_j}{2}, \quad n_{ij} = n_{ji} = \frac{n_i + n_j}{2}, \quad m_{ij} = m_{ji} = \frac{m_i + m_j}{2} \tag{6}$$

$$\varepsilon_{ij} = \varepsilon_{ji} = \sqrt{\varepsilon_i\,\varepsilon_j} \tag{7}$$

Here, *A* is a parameter of length dimension; *m* and *n* are integers having positive values. In this study, K-SC potential parameters used for Pd and Si elements were determined by fitting the experimental parameters such as lattice constant, cohesive energy and bulk modulus. The potential parameters used in the calculations for Pd and Si elements were given as in Table 1 [14].

Table 1. The K-SC potential parameters for Pd and Si elements [14].

Element	*n*	*m*	ε (eV)	*c*	*A* (Å)
Pd	12	7	0,003967	113,14	3,9382
Si	6	5,25	0,064310	12,76	3,7653

In this study, the atoms of the modelled PdSi alloy system were randomly placed at fcc (face-centered cubic) lattice points as their initial positions. Periodic boundary conditions were applied to minimize finite volume effects along three axes of the MD cell. The value of cut-off potential was determined as$2.2A_{PdPd}$. The initial velocities of the atoms were randomly assigned in compliance with the Maxwell-Boltzman distribution at a temperature selected as the starting condition.

By multiplying the atomic velocities by the thermostat parameter in both steps of integration the temperature of the system was kept at the desired value. Gear's 5th order predictor-corrector algorithm was used for the numerical solution of motion equations. The MD computation time was determined as 8.29 fs. By keeping the alloy system along$5x10^4$ MD steps at the temperature value of 2000 K, the structure was allowed to transform completely into the liquid phase. This modelled alloy system balanced in liquid phase was used for all cooling rates and pressures applied. Radial distribution functions are commonly used in MD simulation studies to determine crystal, amorphous and liquid phase structures.

$$g(r) = \frac{V}{N^2}\left\langle \frac{\sum_i n_i(r)}{4\pi r^2 \Delta r} \right\rangle \quad (8)$$

Here, *r* represents the interatomic distance; *n*(*r*) denotes the number of particles in the spherical shell having Δ*r* thickness positioned at the distance of *r* away from *I* atom; *N* is the total number of particles; and *V* expresses the MD cell volume [33].

3. Results

In this study, in order to detect the melting temperature of the PdSi alloy, the temperature of the system was increased by starting from 500K to 2000K by increment steps of 100K. At each temperature value, the system was balancedby$5x10^4$MDsteps. In order to determine the melting temperature, the cohesive energy was plotted against the temperature, as shown in Figure 1. The cohesive energy values were determined by averaging on the last 5000 MD steps for each temperature.

As seen in this plot, the energy increasing linearly with temperature shows a discontinuity when it reaches 1200K. This discontinuity indicates that the modelled alloy system was transformed from a solid phase to a liquid phase. The melting temperature was determined as 1250 ± 50 K from the plot in Figure 1. The experimental melting temperature of the PdSi alloy is 1245K [34]. It is seen that the melting temperature result obtained from MD calculations made for this study is consistent with the experimental values.

After the modelled PdSi alloy system consisting of 4000 atoms gain edits liquid phase structure by having been keptwith$5x10^4$ MD steps at the temperature value of 2000 K, it was cooled down to the temperature of 300 Kat the cooling rates of $2.5x10^{11}$ K/s and $2.5x10^{12}$ K/s and under pressure values of 0, 3 and 7 GPa. The RDF curves for the modelled alloy system at different temperatures obtained at the cooling rate of $2.5x10^{11}$ K/s and under three different pressure values are shown in Figure 2.

It was determined from RDF curves obtained at 1400 K that PdSi alloy had a liquid phase structure under all three pressure values. The same graphs show the splittings one very secondary peak at 700 K for 0 GPa, 800K for 3 GPa and 1000 K for 7 GPa. This splitting on the second peak is known as a characteristic feature of metallic glasses.

The obtained glassy structure has no stable structure. It can be seen from RDF curves where sharper peaks begin to form at different points by decreasing temperature. The peak intensities increased with decreasing temperature and the modelled alloy system has been transformed into a fcc unit cell crystal structure under all three pressure values at 300 K temperature. When the peaks started to form, the nucleation of the crystalline phase began in the liquid phase and the increasing peak intensities with decreasing temperature indicate that the nuclei have been grown and at the end the structure transformed into a crystalline phase [35]. Plus, the inter-atomic distances decreased with increasing pressure caused the peaks shifting to the left.

As shown in Figure 3, the transition temperature of the PdSi alloy system from liquid phase to crystal phase was determined from the cohesive energy change versus temperature for three pressure values. During cooling down from high-temperature, the values decreasing almost linearly showed a sudden discontinuity at certain temperatures. This discontinuity in the cohesive energy refers to the crystallization temperature (T_c), indicating the transition from the liquid phase to the crystal phase [30]. Crystal phase transition temperatures of modelled alloy system were determined as 650 K for 0 GPa, 750 K for 3 GPa and 950 K for 7 GPa of pressure values.

The pressure increment led to an increase in the temperature of transition from liquid phase to crystal phase. Increasing pressure enhanced the density of the modelled alloy system and caused a decrease in the inter-atomic distance. Therefore, it can be said that the pressure increase is a very effective factor in the nucleation and growth of the crystalline phase in the liquid phase [36].

Figure 4 shows the RDF curves obtained by cooling the PdSi alloy system from the liquid phase at the cooling rate of $2.5x10^{12}$K/s. As seen in this figure, while the modelled alloy system was in the liquid phase at the temperature of 1400 K, as a result of the rapid cooling the slumps were appeared to fall to down from the top of the secondary peaks of the RDF curves at the temperature values of 600 K for 0 GPa, 700 K for3 GPa and 900 Kfor7 GPa. By the decrease in temperature this slumps have become more distinct. This slump seen at the secondary peak on the RDF curve shows the transition from the liquid phase to the amorphous structure. It is seen that the modelled alloy system has amorphous phase structure at room temperature in all pressure values. In addition, the primary peak intensity increases with the decrease in temperature in all three pressure cases. It can be said that during the solidification by decreasing temperature, the increase in the close neighbouring order of the atoms in the PdSi alloy caused an increase in the primary peak intensity.

In MD simulations, the Wendt-Abraham parameter is used to determine the glass transition temperature. This parameter is obtained by dividing the first minimum g_{min} value of the RDF curve by the first maximum g_{max} value (g_{min}/g_{max}) [1]. As shown in Figure 5, in order to determine the glass transition temperature of the modelled alloy system the g_{min}/g_{max} change versus temperature was given for different pressure values.

Decreasing almost linearly with decreasing temperature, the g_{min}/g_{max} parameter can be seen to be changed at some temperatures for all three pressure values. The temperature value of this change refers to the glass transition temperature of the modelled alloy system. The glass transition temperature was determined as 600 K, 700 K and 900 K for pressure values of 0 GPa, 3 GPa and 7 GPa, respectively. The increase in pressure applied on the model alloy system increased the glass transition temperature. In previous studies [14, 17] made for different element and alloy systems ,it was also reported that the glass transition temperature had increased by increased pressure. At high pressure values, the distance between the atoms in the liquid phase decreases and the model alloy system gains a higher density. As a result, the decrease in the mobility of atoms due to high pressure increases the T_g value [17].

The reduced glass transition temperature (T_{rg}), known as the ratio of the glass transition temperature to the melting temperature, is a criterion for glass forming ability of alloy systems and can take values from 0.5 to 0.8 [3, 14]. In these MD calculations made here for PdSi alloy system, the T_{rg} values were determined as 0.48 for 0 GPa, 0.56 for 3 GPa and 0.72 for 7 GPa of pressure values. From obtained results, it can be said that the pressure incrementled to an increase in the value of T_{rg} and in the glass forming ability for the cooling rate used.

In Figure 6 (a-c), the positions of the Pd and Si atoms in the modelled alloy system consisting of 4000 atoms can be seen. Figure 6 (a) shows the atomic positions in the modelled alloy system under a pressure of 0 GPa and at a temperature of 2000 K. Since the atoms are completely positioned randomly and irregularly, it can be said that the alloy system is in liquid phase. Figures 6 (b and c) displays the atomic positions obtained at a temperature of 300 K and under the pressure values of 0 GPa and 7 GPa.

At the temperature of 300 K, it is obviously seen that the atoms of the alloy system have a regular arrangement, so it can clearly be concluding that the structure completely transformed into crystal phase from liquid phase. It can also be said that the increase in pressure increased the degree of order of the structure by looking at the atomic positions obtained at the pressure value of 7 GPa.

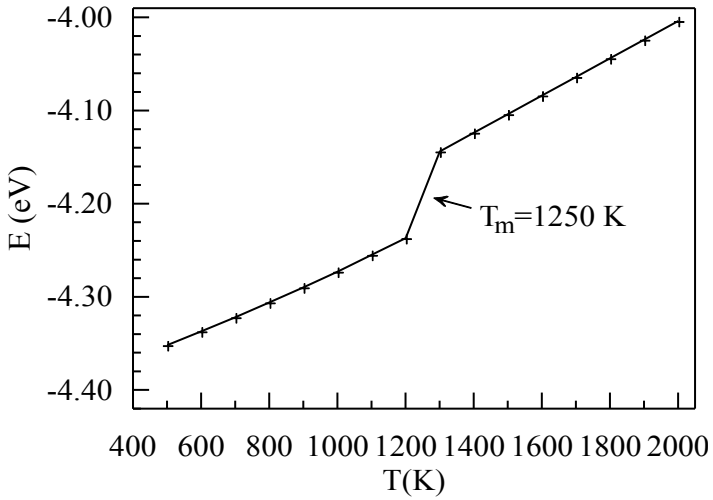

Figure 1. Cohesive energy change versus temperature.

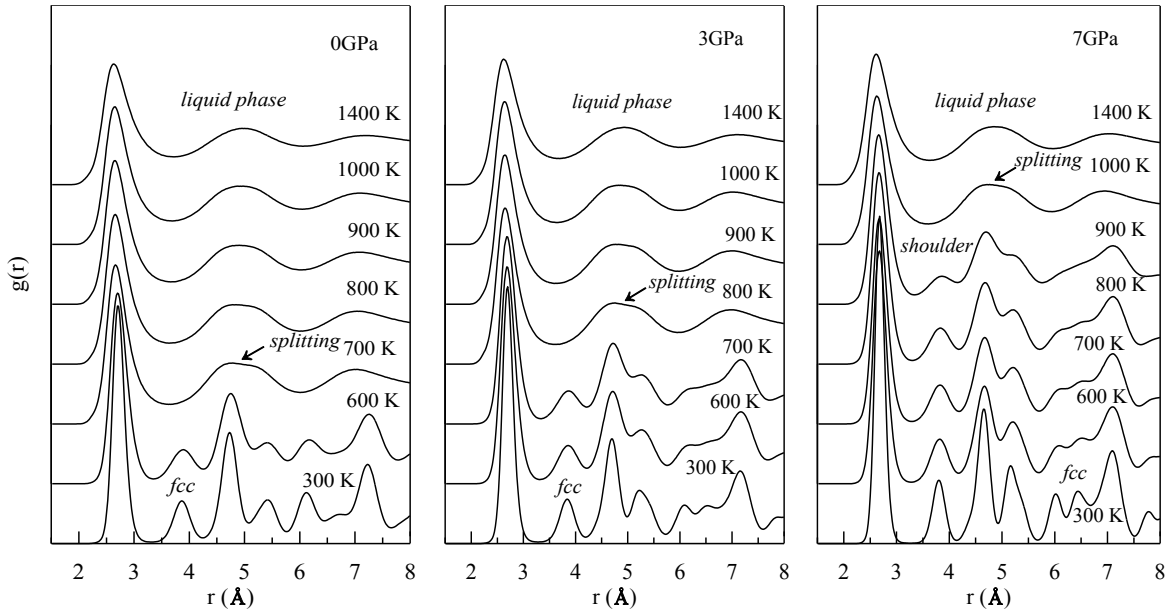

Figure 2. RDF curves obtained for modelled PdSi alloy system under three different pressure values and at the cooling rate of 2.5×10^{11} K/s.

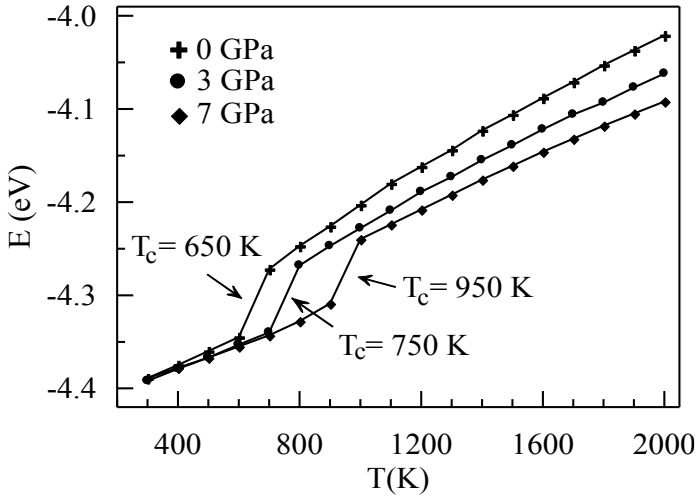

Figure 3. Cohesive energy change versus temperature at the cooling rate of $2.5x10^{11}$ K/s.

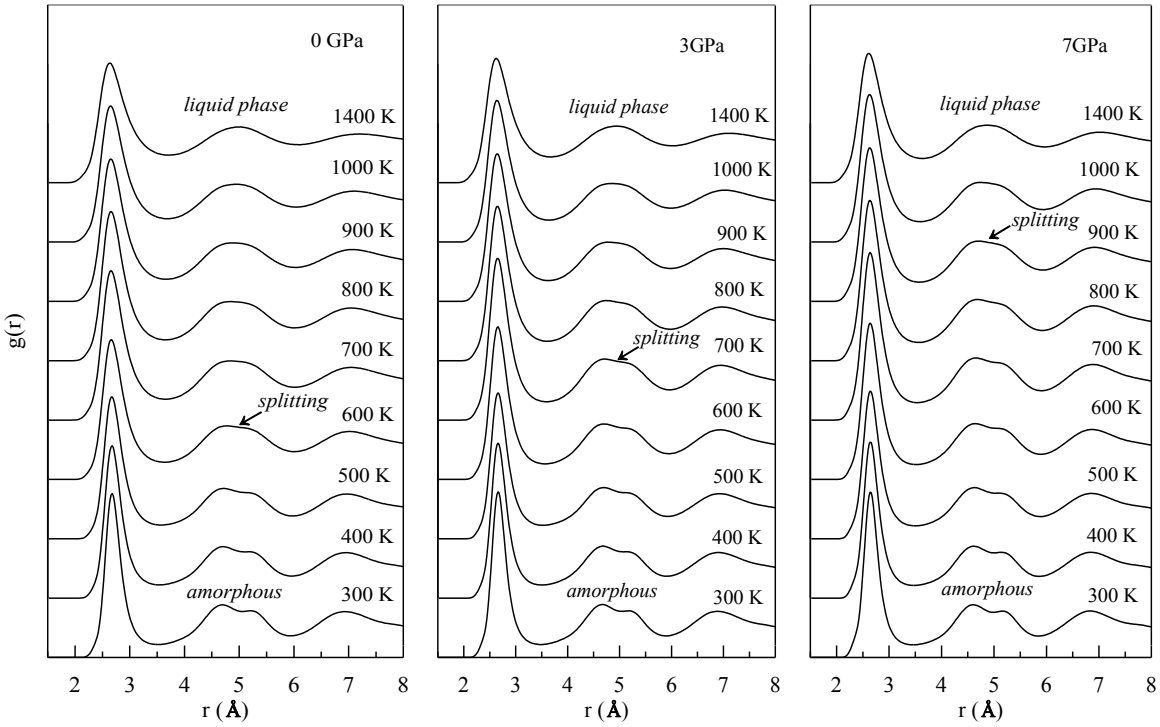

Figure 4: RDF curves obtained for modelled alloy system under three different pressure values and at the cooling rate of $2.5x10^{12}$ K/s.

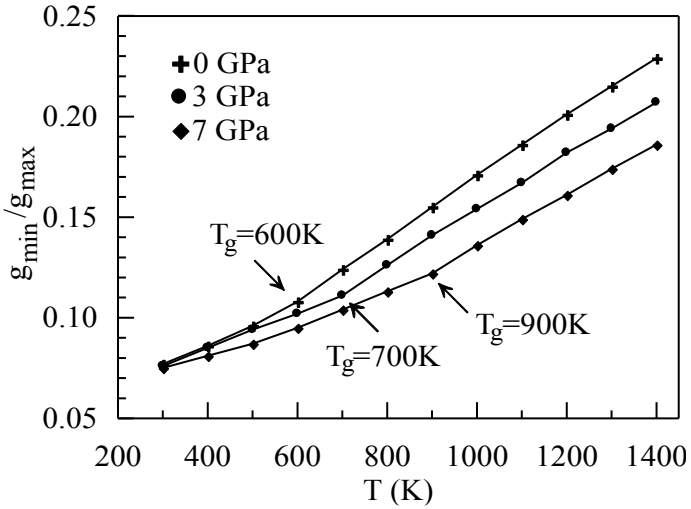

Figure 5. The glass transition temperature under different pressure values and at the cooling rate of $2.5x10^{12}$ K/s.

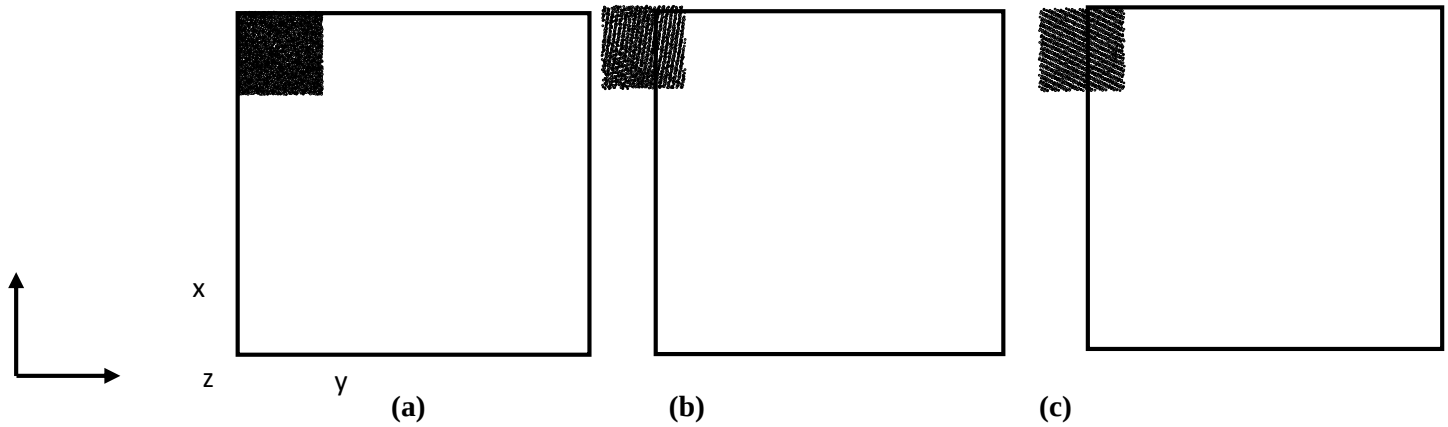

Figure 6. The atomic positions of PdSi alloy system at different temperature and pressure values; (a) 1400 K-0 GPa, (b) 300 K-0 G Pa, (c) 300 K-7 GPa. White spheres show Pd atoms, black spheres show Si atoms.

4. Conclusion

In this work, the effect of pressure on crystallization (T_c) and glass transition temperatures (T_g) of PdSi liquid alloy was investigated for cooling rates of $2{,}5x10^{11}$ K/s and $2{,}5x10^{12}$ K/s. Interactions between atoms were determined by using the Quantum Sutton Chen (K-SC) potential function. It was observed that, the PdSi alloy system was in fcc structure at 300 K temperature under the cooling rate of $2.5x10^{11}$ K/s and in amorphous structure under the cooling rate of 2.5x1012K/s. The glass transition temperature was determined from Wendt-Abraham parameter and radial distribution function (RDF) peaks. By increasing the application pressure on the alloy system the crystallization, glass transition temperature and T_g/T_m ratio increased and the glass formation ability enhanced..

References

[1] Qi L., Zhang H., Hu Z. 2004. Molecular dynamic simulation of glass formation in binary liquid metal: Cu–Ag using EAM. Intermetallics, 12 (10-11): 1191-1195.

[2] Ozgen S., Duruk E. 2004. Molecular dynamics simulation of solidification kinetics of aluminium using Sutton–Chen version of EAM. Materials Letters, 58 (6): 1071-1075.

[3] Wang W.-H., Dong C., Shek C. 2004. Bulk metallic glasses. Materials Science and Engineering: R: Reports, 44 (2-3): 45-89.
[4] Cong H.-R., Bian X.-F., Zhang J.-X., Li H. 2002. Structure properties of Cu-Ni alloys at the rapid cooling rate using embedded-atom method, Materials Science and Engineering: A, 326 (2): 343-347.
[5] Qi L., Zhang H., Hu Z., Liaw P. 2004. Molecular dynamic simulation studies of glass formation and atomic-level structures in Pd–Ni alloy. Physics Letters A, 327 (5-6): 506-511.
[6] Schroers J., Pham Q., Peker A., Paton N., Curtis R.V. 2007. Blow molding of bulk metallic glass. Scripta Materialia, 57 (4): 341-344.
[7] Laws K., Gun B., Ferry M. 2006. Effect of die-casting parameters on the production of high quality bulk metallic glass samples. Materials Science and Engineering: A, 425 (1-2): 114-120.
[8] Busch R., Kim Y., Johnson W. 1995. Thermodynamics and kinetics of the undercooled liquid and the glass transition of the Zr41. 2Ti13. 8Cu12. 5Ni10. 0Be22. 5 alloy. Journal of applied physics, 77 (8): 4039-4043.
[9] Luzzi D., Meshii M. 1986. Criteria for the amorphisation of intermetallic compounds under electron irradiation. Scripta metallurgica, 20 (6): 943-948.
[10] Etemadi R. 2014. Effect of processing parameters and matrix shrinkage on porosity formation during synthesis of metal matrix composites with dual-scale fiber reinforcements using pressure infiltration process. University of Wisconsin Uw milwaukee, Master of Science in Engineering, Master, ABD.
[11] Tuli M., Strutt P.R. 1978. Claitor's Publishing Devision, B. Rouge Louisiana: 113.
[12] Yan M., Sun J.F., Shen J. 2004. Isothermal annealing induced embrittlement of Zr41. 25Ti13. 75Ni10Cu12. 5Be22. 5 bulk metallic glass. Journal of alloys and compounds, 381 (1-2): 86-90.
[13] Xi X.K. 2005. Preparation of Mg-based bulk metallic glasses and their fracture behaviors. Institute of Physics, CAS.
[14] Faruq M., Villesuzanne A., Shao G. 2018. Molecular-dynamics simulations of binary Pd-Si metal alloys: Glass formation, crystallisation and cluster properties. Journal of Non-Crystalline Solids, 487: 72-86.
[15] Hui L., Pederiva F. 2004. Structural study of local order in quenched lead under high pressures. Chemical physics, 304 (3): 261-271.
[16] Wang Z., Wang R., Wang W. 2006. Elastic properties of Cu60Zr20Hf10Ti10 bulk metallic glass under high pressure. Materials Letters, 60 (6): 831-833.
[17] Shimojo F., Hoshino K., Zempo Y. 2002. Intermediate-range order in liquid and amorphous As2S3 by ab initio molecular-dynamics simulations. Journal of non-crystalline solids, 312: : 388-391.
[18] Çağın T., Dereli G., Uludoğan M., Tomak M. 1999. Thermal and mechanical properties of some fcc transition metals. Physical Review B, 59 (5): 3468.
[19] Zhang X.-J., Chen C.-L. 2012. Phonon dispersion in the Fcc metals Ca, Sr and Yb. Journal of Low Temperature Physics, 169 (1-2): 40-50.
[20] Tolpin K., Bachurin V., Yurasova V. 2012. Features of energy dependence of NiPd sputtering for various ion irradiation angles. Nuclear Instruments and Methods in Physics Research Section B: Beam Interactions with Materials and Atoms, 273: 76-79.
[21] Louail L., Maouche D., Roumili A., Hachemi A. 2005. Pressure effect on elastic constants of some transition metals. Materials chemistry and physics, 91 (1): 17-20.
[22] Pelaz L., Marqués L. A., Aboy M., López P., Barbolla J. 2005. Atomistic modeling of dopant implantation and annealing in Si: damage evolution, dopant diffusion and activation. Computational materials science, 33 (1-3): 92-105.
[23] Shao Y., Clapp P.C., Rifkin J. 1996. Molecular dynamics simulation of martensitic transformations in NiAI. Metallurgical and Materials Transactions A, 27 (6): 1477-1489.
[24] Daw M. S., Hatcher R. 1985. Application of the embedded atom method to phonons in transition metals. Solid state communications, 56 (8): 697-699.
[25] Voter A.F., Chen S.P. 1986. Accurate interatomic potentials for Ni, Al and Ni3Al. MRS Online Proceedings Library Archive, 82: 175.
[26] Finnis M., Sinclair J. 1984. A simple empirical N-body potential for transition metals. Philosophical Magazine A, 50 (1): 45-55.

[27] Sutton A., Chen J. 1990. Long-range finnis–sinclair potentials. Philosophical Magazine Letters, 61 (3): 139-146.
[28] Grujicic M., Dang P. 1995. Computer simulation of martensitic transformation in Fe-Ni face-centered cubic alloys. Materials Science and Engineering: A, 201 (1-2): 194-20.
[29] Gui J., Cui Y., Xu S., Wang Q., Ye Y., Xiang M., Wang R. 1994. Embedded-atom method study of the effect of the order degree on the lattice parameters of Cu-based shape memory alloys. Journal of Physics: Condensed Matter, 6 (24): 4601.
[30] Caprion D., Schober H. 2003. Computer simulation of liquid and amorphous selenium. Journal of non-crystalline solids, 326: 369-373.
[31] Parrinello M., Rahman A. 1980. Crystal structure and pair potentials: A molecular-dynamics study. Physical Review Letters, 45 (14): 1196.
[32] Parrinello M., Rahman A. 1981. Polymorphic transitions in single crystals: A new molecular dynamics method. Journal of Applied physics, 52 (12): 7182-7190.
[33] Rigby M., Maitland G.C., Smith E.B., Wakeham W.A. 1986. The forces between molecules,T144, Oxford University Press, Clarendon Press.
[34] Baxi H., Massalski T. 1991. The pdsi (palladiumsilicon) system. Journal of phase equilibria, 12 (3): 349-356.
[35] Wang L., Peng C., Wang Y., Zhang Y. 2006. Relating nucleation to dynamical and structural heterogeneity in supercooled liquid metal. Physics Letters A, 350 (1-2): 69-74.
[36] Shimono M., Onodera H. 2001. Molecular dynamics study on formation and crystallization of Ti–Al amorphous alloys. Materials Science and Engineering: A, 304: 515-519.